Risø National Laboratory

Postprint

Multiple scattering effects in laser ablation plume propagation in gases

Salvatore Amoruso1, Jørgen Schou2 and James G. Lunney3

1Coherentia-INFM and Dipartimento di Scienze Fisiche, Università degli Studi Federico II,
Complesso Universitario di Monte S. Angelo, Via Cintia, I-80126 Napoli, Italy.
2OPL, Risø National Laboratory, DK-4000 Roskilde, Denmark
3School of Physics, Trinity College, Dublin 2, Ireland

Multiple scattering effects in laser ablation plume propagation in gases

Salvatore Amoruso[1], Jørgen Schou[2] and James G. Lunney[3]

[1]*Coherentia-INFM and Dipartimento di Scienze Fisiche, Università degli Studi Federico II,*
Complesso Universitario di Monte S. Angelo, Via Cintia, I-80126 Napoli, Italy.
[2]*OPL, Risø National Laboratory, DK-4000 Roskilde, Denmark*
[3]*School of Physics, Trinity College, Dublin 2, Ireland*

Abstract. - Langmuir probe technique has been employed to characterize the dynamics of UV laser ablation plasma ions from a silver target in different background gases (He, Ne, Ar and Xe). For all these gases the ion time-of-flight signals show progressive formation of a slower component as the gas pressure is increased. In the case of heavier gases (Ar and Xe) this slower component is clearly resolved from the *vacuum peak* (plume splitting), as has been previously reported. The pressure variation of the collected ion yield deviates markedly from a simple exponential decay, and a new approach, based on multiple elastic scattering processes, has been developed to describe these results as well as to provide elastic collision cross sections which were previously not available. For the heavier gases, it has been possible to analyze the two ion components separately, and to estimate both the elastic collision cross sections and the scattering order for the different gases.

PACS number(s): 52.38.Mf, 79.20.Ds, 81.15.Fg

Short title: Multiple scattering effects in laser ablation

Introduction. - The physics of laser ablation in background gases continues to receive much attention due to its importance in a number of techniques, such as pulsed laser deposition (PLD) of thin films and nanoparticle formation [1,2]. Further development of these techniques requires a better understanding of the mechanisms of laser-solid interaction, plasma plume formation, and plume expansion in vacuum or in gaseous atmospheres. In particular, it is of interest to examine how the nature and the pressure of the background gas influence the propagation of the ablation plume. Except for the modeling of the propagation of a silicon plume in He and Ar [3,4], and an aluminum plume in O_2 [5], there exists no satisfactory description of the propagation of an ablation plume in a background gas over a wide range of pressure.

The plume expansion dynamics depends strongly on the atomic/molecular mass and pressure of the background gas. In a certain gas pressure range time-of-flight (TOF) ion signals are observed to split into two components; an attenuated vacuum-like signal plus a separate signal at longer time [3,4,6,7]. For the case of silicon ablation in He and Ar, model calculations have shown that this *plume splitting* can be interpreted in terms of the multiple scattering dynamics of the plume particles by the background [3,4]. A combined continuum-microscopic method has been used to model the propagation of a metal plume in oxygen [5]. While these numerical models do reveal some aspects of the complexity and underlying processes involved in plume expansion in gas, the results refer to specific target/gas systems and cannot easily be used for the interpretation of experimental results for other materials and ablation conditions.

In this letter, a new, simple analytical approach based on multiple scattering is described and applied to the experimental data on propagation of an Ag laser ablation plume in several inert background gases (He, Ne, Ar and Xe). Time-resolved Langmuir probe technique was used to measure the dependence of the collected ion flux on the background gas pressure.

This allows the identification of the different regimes of plume expansion, from effectively free expansion at low pressure, through a regime of multiple scattering at intermediate pressure, to blast wave propagation and finally to diffusive-like transport at relatively high pressure. In our simple approach we do not include angular scattering, but consider a sequence of energy loss events. Our analytical multiple scattering theory is remarkably successful in describing quantitatively the ion flux data and clearly identifies the role of multiple scattering without requiring extensive numerical modelling. Moreover, it yields an estimate of both the elastic collision cross section and the scattering order for the different gases.

Experimental setup. - The experiments were carried out using a setup at Risø National Laboratory, which has been described earlier [8-11]. A frequency-tripled Nd:YAG laser beam (λ=355 nm, pulse width $\approx$6 ns FWHM, laser fluence $\approx$2.5 Jcm^{-2}) was directed at normal incidence onto a circular 0.04 cm^2 spot on a silver target in a vacuum chamber with a base pressure of 10^{-7} mbar. The ion flux was measured by using a planar Langmuir probe oriented to face the target spot and located at a distance of 75 mm from the target and at an angle of $\approx$20^{o} with respect to the normal of the target surface. The probe collecting area was a 2$\times$2 mm^2 square copper plate insulated on the rear side, similarly to refs 9-10. During the ion collection the probe was biased at $-$10 V. A sketch of the experimental configuration is shown as inset in Fig. 1(a). The ablation leads to the removal of about 700 ng per pulse of material which expands into vacuum as a forward-peaked plume with a longitudinal to transverse aspect ratio of 2.8 [11]. The total number of ions in the plume is 1$\times$10^{15} Ag ions per shot at 2 J/cm^2 [12].

Results. - The experimental results for He and Xe are given in Fig. 1, where (a) and (b) show the TOF distributions measured by the ion probe for several representative values of the gas pressure. Figure 1(c) and 1(d) show the pressure dependence of the total ion flux, obtained by integrating the TOF profiles, for He and Xe, respectively.
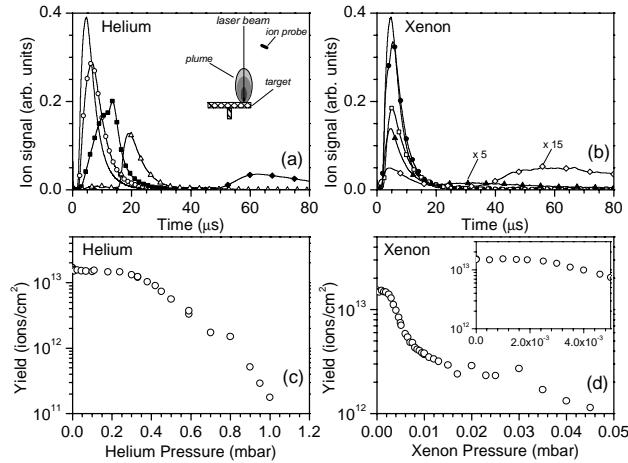

Fig. 1 - Ion probe measurements in He and Xe. Representative TOF profiles are shown in (a) helium: vacuum (full line), 1×10^{-1} mbar ($\circ$), 3×10^{-1} mbar ($\blacksquare$), 4.5×10^{-1} mbar(Δ); 5.9×10^{-1} mbar ($\blacklozenge$) and (b) xenon: vacuum (full line), 1.2×10^{-5} mbar ($\bullet$), 5×10^{-3} mbar ($\square$), 1.0×10^{-2} mbar ($\blacktriangle$); 2.0×10^{-2} mbar ($\lozenge$). The pressure dependence of the integrated ion flux is shown for helium (c) and xenon (d). The inset in (a) shows a sketch of the experimental setup and the inset in (d) shows an expanded view of the xenon data at low pressures.

Considering first the results for He [Fig. 1 (a) and (c)], we can see that: (i) from vacuum up to ≈0.2 mbar the total ion flux reaching the probe is almost constant, and the TOF profile broadens while being slightly delayed; (ii) above 0.3 mbar the ion flux starts decreasing and a peak appears on the trailing edge of the TOF signal; (iii) at still larger pressures this delayed peak becomes dominant indicating that nearly all of the ions reaching the probe have been delayed with respect to the vacuum case, while the collected flux continues to fall with increasing pressure. The results for Xe [Fig. 1 (b) and (d)] reveal a somewhat different dynamical behaviour. The integrated ion signal is constant up to ≈3×10^{-3} mbar as shown in the inset in Fig. 1(d). Thereafter the ion signal decreases with increasing pressure but the time profile is hardly changed, except for the appearance of a shoulder on the trailing edge of the

pulse. This shoulder progressively transforms into a second, delayed peak for pressures larger

than 1.0×10^{-2} mbar, which becomes dominant above $\approx 2.0 \times 10^{-2}$ mbar. As compared to He, a

distinctly different behavior can be recognized in the pressure variation of the integrated ion

flux in Xe shown in Fig. 1(d). These behaviors originate from the complex interplay between

the two components into which the ion flux is split for plume propagation in a certain range of

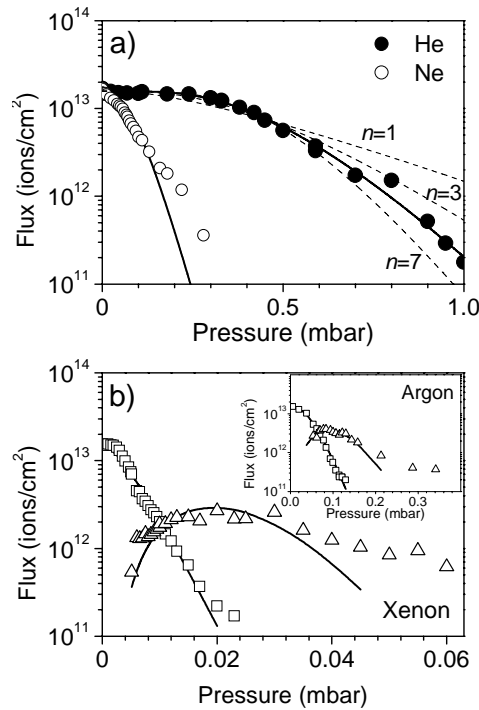gas pressure [7,11], as will be discussed next.

Fig. 2 - Pressure variation of (a) net ion flux for He and Ne and (b) fast (□) and slow (Δ) ion peaks pressure for Xe and Ar (inset). The solid lines are theoretical fits (see text for details). In panel (a), the dashed curves show fits according to Eq. (3) for different values of the maximum scattering order n, in the case of He.

The experimental observation of a plateau in the collected ion flux Y at low pressures

indicates that a simple Beer's law type behaviour, $Y(x_D) = Y_0 \exp(-x_D/\lambda)$, that might be

expected for hard-sphere, elastic scattering from fixed scattering centres, is not valid, x_D being

the target-detector distance, λ the mean free path and Y_0 the ion-flux collected in high

vacuum. Since $\lambda = 1/(\sqrt{2} n_g \sigma_c) \propto P^{-1}$, Beer's law behavior would give an exponential

reduction of ion signal with pressure P (where σ_c is the scattering cross section and n_g the gas density). While the assumption of fixed scattering centres is not completely valid for the collision of Ag ions with the relatively light He, the observation of a similar behaviour also for the heavier gases Ne, Ar, and Xe points to a general feature of the process of plume propagation in a background gas. The observed behaviour can be understood if one considers that in addition to the fraction of ions reaching the detector without collision (ballistic component), there is an additional contribution from ions that have suffered one, or more, collisions (multiple scattering). It is an analytical description of this multiple scattering which is the essential feature of our theoretical approach.

Thus the number of ions collected by the probe has two contributions: (i) a ballistic component, F_b and (ii) a scattered component F_s, which can be further separated into fractions which have undergone 1, 2, 3, k scattering events. Therefore, the number of particles reaching the detector, Y_D, is given by:

(1) $$Y_D = Y_0(F_b + F_s) = Y_0(F_b + F_1 + F_2 + ... + F_k + ...)$$

where F_k is the fraction collected after k scattering events. The evaluation of Y_D is a very complex problem, which can be treated analytically only by considering the following approximations: (i) the real path of the ion can be approximated to a straight line joining the ablation spot on the target and the detector; (ii) the maximum order of scattering is low, i.e. F_k decreases very strongly with the scattering order k. In such a case, if l_i denotes the path length travelled by the particles between the (i-1)-th and i-th scattering events, for a particle having suffered k collisions we get $\sum_{i=1}^{k+1} l_i \approx x_D$, where l_{k+1} denotes the length of the path going from the point where the k-th scattering occurs to the detector. Under these assumptions, the evaluation of F_k reduces to a one-dimensional problem, i.e. we neglect angular scattering, and the number of terms in Eq. (1) is small. The probability, $\Pi_k(\mu, \lambda)$, that an ion will

experience k collisions along a total path of length of the order of x_D is described by the Poisson distribution given by:

(2)
$$\Pi_k(\mu,\lambda) = \mu^k \frac{e^{-\mu}}{k!} = \left(\frac{x_D}{\lambda}\right)^k \frac{e^{-\frac{x_D}{\lambda}}}{k!} = \left(\frac{P}{P_0}\right)^k \frac{e^{-\frac{P}{P_0}}}{k!}$$

where $\mu = x_D/\lambda$. The number of ions reaching the probe having undergone up to n collisions is given by:

(3)
$$Y_D(P) = Y_0 e^{-\frac{P}{P_0}} \sum_{k=0}^{n} \frac{1}{k!} \left(\frac{P}{P_0}\right)^k$$

where $P_0 = k_B T_{amb}/\sqrt{2}\sigma_c x_D$, k_B and T_{amb} being the Boltzmann constant and the ambient temperature, respectively. Thus $\sigma_c (cm^2) = 3.9\times10^{-18}/P_0 (mbar)$.

Fig. 2(a) shows the ion flux for He and Ne and fits according to Eq. (3). The procedure has been carried out by progressively increasing the value of the maximum scattering order n until a good fit is achieved, and using Y_0 and P_0 as fitting parameters. As shown in Fig. 2(a) for He, the shape of the fitting curve depends strongly on n, and a good convergence over a large range of pressure is only attained for a specific value. Therefore, this analysis does provide us with a fairly accurate value of the maximum scattering order. The value of Y_0 is determined by the integrated ion flux collected in high vacuum ($\approx 1.5\times10^{13}$ ions/cm^2). Using the fitted value of P_0, the collision cross section is estimated. The values of n and σ_c are summarized in table I.

For Ar and Xe background, it is possible to analyze the behavior for the fast and slow peaks separately. The collected ion yield of the fast and slow peaks in Xe and Ar is shown in Fig. 2(b). As discussed below, the second peak is determined by a completely different mechanism. The ion yield of the fast peak (open squares), is nearly constant up to $\approx 3\times10^{-3}$ mbar for Xe, and $\approx 3\times10^{-2}$ mbar for Ar. The pressure variation of the ion yield in the fast peak

has been fitted to Eq. (3) using the same procedure as for He and Ne. It should be noted since Xe is heavier than Ag some of the Ag ions will be backscattered, which is not the case for the other gases in this experiment. By analyzing the phase function for scattering of Ag and Xe we estimated that ≈18% of collisions lead to backscattering. This fraction of the incoming flux is considered lost after each collision and is taken into account in the fitting procedure and derivation of the collision cross section. From Fig. 2(b) it is apparent that the theoretical fits reproduce closely the experimental data for the first peak, yielding the values of n and σ_c reported in table I. The estimate of the fits coincides with our expectation that Ar, with a lower atomic radius and mass will have a smaller collision cross section and require more collisions for the same degree of slowing, as compared to Xe. The good agreement of the theoretical curves in Fig. 2 with the experimental data clearly suggests that the essential physics underlying plume propagation in gas is described by our simplified multiple scattering theory.

The values of σ_c obtained by our multiple scattering model are consistent with the order of magnitude of the 'atomic cross section' πa_0^2 (=0.88×10^{-16} cm^2), a_0 being the Bohr radius. The observed increase for the larger atoms of the background gas can be accounted for by a simple kinetic theory approach evaluating the elastic cross section as $\pi\left(R_p + R_t\right)^2$, R_p and R_t being the radius of the projectile and target particles, respectively. By approximating R_p and R_t to the covalent radius of the atoms [13], we obtain values of the elastic cross section (see table I) which result in a fairly good agreement with the values previously obtained by fits of the experimental data to Eq.(3).

It is of interest to examine the pressure dependence of the number of ions in the second peak reaching the probe, as is shown by open triangles in Fig 2. We observe that the second peak yield initially increases with the pressure, reaches a maximum and then falls as the

pressure increases further. The slower peak is due to the propagation of a blast wave in the gas [7,14]. This blast wave is driven by the sudden release of energy in the gas near the laser spot on the target by collision of ablation plume particles with gas atoms. The rise of the second peak yield occurs mainly by transfer of ions from the fast to the slow peak through collisions with the gas. This transfer of ions is not included directly in our model, but we note that an ion will be lost from the fast peak and transferred to the blast wave peak when it has suffered sufficient collisions to reduce its velocity to the local value of the blast wave velocity. Thus is possible to use our multiple collision model to analyse the pressure variation of the second peak and estimate the number of collisions that particles in that peak have encountered.   As the pressure is increased still further less and less of the ions in the delayed part of the plume reach the probe, instead they are trapped within a nearly hemispherical blast wave which expands into the gas in a manner which has been widely discussed in the literature [11,12,15,16]. Eventually the finite pressure of the background gas halts the expansion of the blast wave, and Ag ions can only reach the probe by diffusion [11, 16]. The blast wave and diffusion regimes correspond to the range of pressure with a progressive attenuation of the number of ions in the slow peak reaching the probe, but this will not be discussed here [11]. Instead we will focus on a theoretical interpretation of the early part of the pressure dependence of the slow peak; namely the rising edge and maximal region.

Table I - Maximum scattering order n and collision cross section σ_c obtained by fits of the experimental data for the fast peak yield to Eq. (3). The covalent radius of the gases and the theoretical elastic cross section are also reported for comparison. The covalent radius of Ag is 1.53 Å [13]. See text for details.

Gas	n	Covalent radius (Å)	σ_c (10^{-16} cm^2)	
			experimental	*theoretical*
He	5	0.32	≈ 0.5	≈ 0.4
Ne	3	0.69	≈ 1.7	≈ 1.6
Ar	3	0.97	3.1	≈ 3.1
Xe	1	2.3	12	≈ 17

In the multiple scattering regime, the ion yield $Y_{2nd}(\lambda)$ in the second peak is described by summing up those ion fractions belonging to orders larger than the maximum scattering order n included in the fit for the first peak, i.e.:

(4)
$$Y_{2nd}(\lambda) = Y_0 e^{-\frac{P}{P0}} \sum_{k=k-\min}^{k-\max} \frac{1}{k!}\left(\frac{P}{P_0}\right)^k$$

with k-min$>n$. From Equation (4) it can be seen that the ion signal due to a particular scattering order k will be maximized a pressure $P_{\max} = kP_0$. The pressure where the slow peak is maximized corresponds to k values of ≈ 7 in Ar and ≈ 4-5 in Xe. Equation (5) has been used to fit the pressure dependence of the measured ion yield in the second peak for Ar and Xe using the same scattering cross sections as for the fast peak, and is shown in Fig. 2(b). As before, a backscattered fraction of $\approx 18\%$ was included in fitting the Xe case. From these fits we obtain (k-min, k-max) is (4-11) for Ar and (4-10) for Xe, again showing that in the heavier gas a smaller number of scattering orders is required for the same degree of ion slowing. Secondly we note that the values of Y_0 used in the fitting are 4.3×10^{12} and 3.6×10^{12} ion/cm^2, which is lower than the values of integrated ion flux in vacuum. We can expect some reduction in the value of Y_0 associated with the second peak due to the combined effect of electron-ion recombination and non-head-on collisions tending to make the plume more hemispherical compared to the vacuum case. Thus it seems that the data fits in Fig. 2(b) do allow us conclude that our multiple scattering approach gives a reasonable description of the slow peak, at least in the pressure regime where it first appears.

The dilution of the background gas by collisions is not a major issue. For instance, if we consider that the ion flux at the probe position (7.5 cm from the target) is $\approx 1.5 \times 10^{13}$ ions/cm^2, we can estimate a flux of the order of $\approx 10^{15}$ ions/cm^2 at a distance of ≈ 1 cm from the target surface. From the estimated cross sections (see table I), for example in the case of Ar, we obtain a probability that a background gas atom suffers a collision with an Ag ion

from the plume of ≈ 0.3. Therefore only a fraction of the order of $\approx 30\%$ of the background gas atoms is involved in collisions at a distance of ≈ 1 cm from the target surface. Since the probability of a collision is proportional to the ion flux, which roughly drops off as d^2, where d is the distance from the target, we can conclude that beyond about 1 cm from the target only a minor fraction of the background gas is driven out of the interaction volume.

Conclusion. - The dynamics of UV laser ablation plasma ions from a silver target in different background gases has been studied by Langmuir probe technique. A new approach, based on multiple elastic scattering processes, has been developed to describe the observed dependence of the ion flux on the background gas pressure, resulting in good agreement with the experimental data. It seems that this multiple scattering approach works well up to pressures where the target-detector distance corresponds to 5-10 mean free paths, depending on the target material and gas. At higher pressures it is necessary to consider blast wave and ion diffusion effects. Finally, it is worth observing that during these experiments the total flux (ions+neutrals) as measured by deposition on a nearby quartz crystal microbalance shows the same behavior [11,17]. We observed that the ion yield exhibits the same pressure dependence as the deposition rate over many orders of magnitude, indicating that the processes discussed in this letter represent the overall dynamics of the ablation plume. Thus our multiple scattering approach to laser ablation plume propagation in background gases should prove useful for the interpretation of a range of laser ablation experiments.

REFERENCES

[1] CHRISEY D.B. and HUBLER G.K. (Eds.), *Pulsed Laser Deposition of Thin Films* (Wiley Interscience, New York) 1994.

[2] BÄUERLE D., *Laser Processing and Chemistry* (Springer, Berlin) 2000.

[3] WOOD R.F., CHEN K.R., LEBOEUF J.N., PURETZKY A.A., and GEOHEGAN D.B., *Phys. Rev. Lett.*, **79** (1997) 1571.

[4] WOOD R.F., LEBOEUF J.N., GEOHEGAN D.B., PURETZKY A.A., and CHEN K.R., *Phys. Rev. B*, **58** (1998) 1533.

[5] ITINA T.E., HERMANN J., DELAPORTE P., and SENTIS M., *Phys. Rev. E*, **66** (2002) 066406.

[6] AMORUSO S., TOFTMANN B., SCHOU J., VELOTTA R. and WANG X, *Thin Solid Films*, **453-454** (2004) 562.

[7] SCHOU J., AMORUSO S. and LUNNEY J.G., in: *Laser ablation and its applications,* ed. PHIPPS C. (Springer-Verlag, Berlin-Heidelberg, 2006) pp. 69-97

[8] HANSEN T.N., SCHOU J. and LUNNEY J.G., *Europhys. Lett.*, **40** (1997) 441-446.

[9] HANSEN T. N., SCHOU J. and LUNNEY J.G., *Appl. Phys. Lett.*, **72** (1998) 1829.

[10] TOFTMANN B., SCHOU J., HANSEN T.N., and LUNNEY J.G., *Phys. Rev. Lett.*, **84** (2000) 3998.

[11] AMORUSO S., TOFTMANN B., SCHOU J., *Phys. Rev. E,* **69** (2004) 056403.

[12] THESTRUP B., TOFTMANN B., SCHOU J., DOGGETT B. and LUNNEY J.G., *Appl. Surf. Sci.*, **197-198** (2002) 175.

[13] JAMES A.M. and LORD M.P., in *Macmillan's Chemical and Physical Data* (Macmillan, London, UK) 1992.

[14] SEDOV L. I., *Similarity and Dimensional Methods in Mechanics* (CRC Press, Boca Raton, FL) 1993.

[15] AMORUSO S., BRUZZESE R., SPINELLI N., VELOTTA R. VITIELLO M. and WANG X., *Phys. Rev. B*, **67** (2003) 224503.

[16] NAKATA Y., KALBARA H., OKADA T. and MAEDA M., *J. Appl. Phys.*, **80** (1996) 2458.

[17] TOFTMANN B., AMORUSO S., SCHOU J., and LUNNEY J. G., in preparation.